Protein Engineering vol.14 no.11 pp.943–948, 2001

Sucrose transport through maltoporin mutants of *Escherichia coli*

Patrick Van Gelder[1,2,3], Raimund Dutzler[1,4], Fabrice Dumas[1,5], Ralf Koebnik[2,6] and Tilman Schirmer[1,7]

[1]Division of Structural Biology and [2]Division of Microbiology, Biozentrum, University of Basel, Klingelbergstrasse 50, CH-4056 Basel, Switzerland

[3]Present address: Dienst Ultrastructuur, Vlaams Interuniversitair Instituut voor Biotechnologie, Vrije Universiteit Brussel, Paardenstraat 65, B-1640 Sint-Genesius-Rode, Belgium
[4]Present address: Laboratory of Molecular Neurobiology and Biophysics, The Rockefeller University, 1230 York Avenue, New York, New York 10021, USA
[5]Present address: IPBS, CNRS, 205 route de Narbonne, 31077 Toulouse, France
[6]Present address: Martin Luther University, Institute of Genetics, D-06099 Halle (Saale), Germany

[7]To whom correspondence should be addressed.
E-mail: tilman.schirmer@unibas.ch

Maltoporin (LamB) and sucrose porin (ScrY) reside in the bacterial outer membrane and facilitate the passive diffusion of maltodextrins and sucrose, respectively. To gain further insight into the determinants of solute specificity, LamB mutants were designed to allow translocation of sucrose, which hardly translocates through wild-type LamB. Three LamB mutants were studied. (a) Based on sequence and structure alignment of LamB with ScrY, two LamB triple mutants were generated (R109D, Y118D,D121F; R109N,Y118D,D121F) to mimic the ScrY constriction. The crystal structure of the first of these mutants was determined to be 3.2 Å and showed an increased ScrY-like cross-section except for D109 that protrudes into the channel. (b) Based on this crystal structure a double mutant was generated by truncation of the two residues that obstruct the channel most in LamB (R109A,Y118A). Analysis of liposome swelling and *in vivo* sugar uptake demonstrated substantial sucrose permeation through all mutants with the double alanine mutant performing best. The triple mutants did not show a well-defined binding site as indicated by sugar-induced ion current noise analysis, which can be explained by remaining steric interference as deduced from the crystal structure. Binding, however, was observed for the double mutant that had the obstructing residues truncated to alanines.

Keywords: current fluctuation analysis/LamB/porin/ScrY/sugar transport

Introduction

The outer membrane of Gram-negative bacteria consists of an asymmetric bilayer with phospholipids constituting the inner leaflet and lipopolysaccharides (LPS) in the outer leaflet. This membrane provides an impermeable barrier for hydrophilic solutes. Uptake of nutrients through this barrier is accomplished by several pore forming proteins (Nikaido and Vaara, 1985). In addition to the general diffusion porins which discriminate solutes primarily according to size (<600 Da) and charge, channels with specificity for certain solutes are present in the outer membrane (Koebnik *et al.*, 2000).

The maltooligosaccharide-specific channel LamB or maltoporin of *Escherichia coli* is the best characterized porin. LamB is expressed as part of the *mal*-regulon upon induction by maltose or maltodextrins (Szmelcman and Hofnung, 1975; Szmelcman *et al.*, 1976) and serves as the receptor for bacteriophage lambda (Randall-Hazelbauer and Schwartz, 1973). Liposome swelling assays showed that maltoporin has a high permeation rate for maltose and maltodextrins whereas uptake of sucrose could hardly be detected (Luckey and Nikaido, 1980; Hardesty *et al.*, 1991). In contrast to this, both maltose and sucrose exhibit similar binding affinities (10 mM for maltose and 15–6 mM for sucrose) to the maltoporin channel as determined by inhibition of ion flow in planar lipid bilayers (Schülein *et al.*, 1991; Andersen *et al.*, 1995). The crystal structure of LamB (Schirmer *et al.*, 1995) and of several LamB–sugar complexes (Dutzler *et al.*, 1996; Wang *et al.*, 1997) are known. The monomer consists of an 18 stranded β-barrel with short turns at the periplasmic side and large irregular loops at the extra cellular side. Loops L1 and L6 are located inside the outer vestibule of the channel. The third loop, L3, folds inside the β-barrel, thereby forming a constriction at the middle of the channel (Figure 1a). An elongated apolar patch composed of aromatic residues ('greasy slide') extends from the extracellular vestibule to the periplasmic exit. Maltodextrins (Dutzler *et al.*, 1996) and the glucosyl residue of sucrose (Wang *et al.*, 1997) are found at van der Waals distances to the greasy slide. Additionally, the sugar hydroxyls interact with several ionic residues (Dumas *et al.*, 2000). Whereas maltodextrins bind to the middle of the channel, sucrose appears stuck above the channel constriction owing to its bulky fructosyl residue. This observation explains how sucrose can inhibit ion flow, although it does not permeate.

A sucrose-specific porin (ScrY of *Salmonella typhimurium*), which is part of a plasmid encoded regulon, has been identified and found to be homologous to LamB (Schmid *et al.*, 1988; Hardesty *et al.*, 1991). Cells containing this plasmid are able to grow on sucrose as the sole carbon source (Schmid *et al.*, 1991; Hardesty *et al.*, 1991). ScrY reconstituted into vesicles showed a high permeation rate for sucrose, but no permeation of maltose (Hardesty *et al.*, 1991). *In vivo* ^{14}C-labelled maltopentaose was not taken up quickly by cells expressing only ScrY as pore protein (Schülein *et al.*, 1995), whereas growth was possible on maltotetraose (Schmid *et al.*, 1991). Recently, the crystal structure of ScrY has been elucidated (Forst *et al.*, 1998). Although the sequence identity is only 20%, the trimeric structures are highly similar. In particular, the greasy slide and other residues of the channel lining are largely conserved (Figure 1a). There are, however, three substitutions at the pore constriction (residues R109, Y118, D121 of LamB corresponding to N192, D201 and F204 of ScrY) which confer a larger cross-section to the ScrY channel constriction. Noteworthy, these residues also

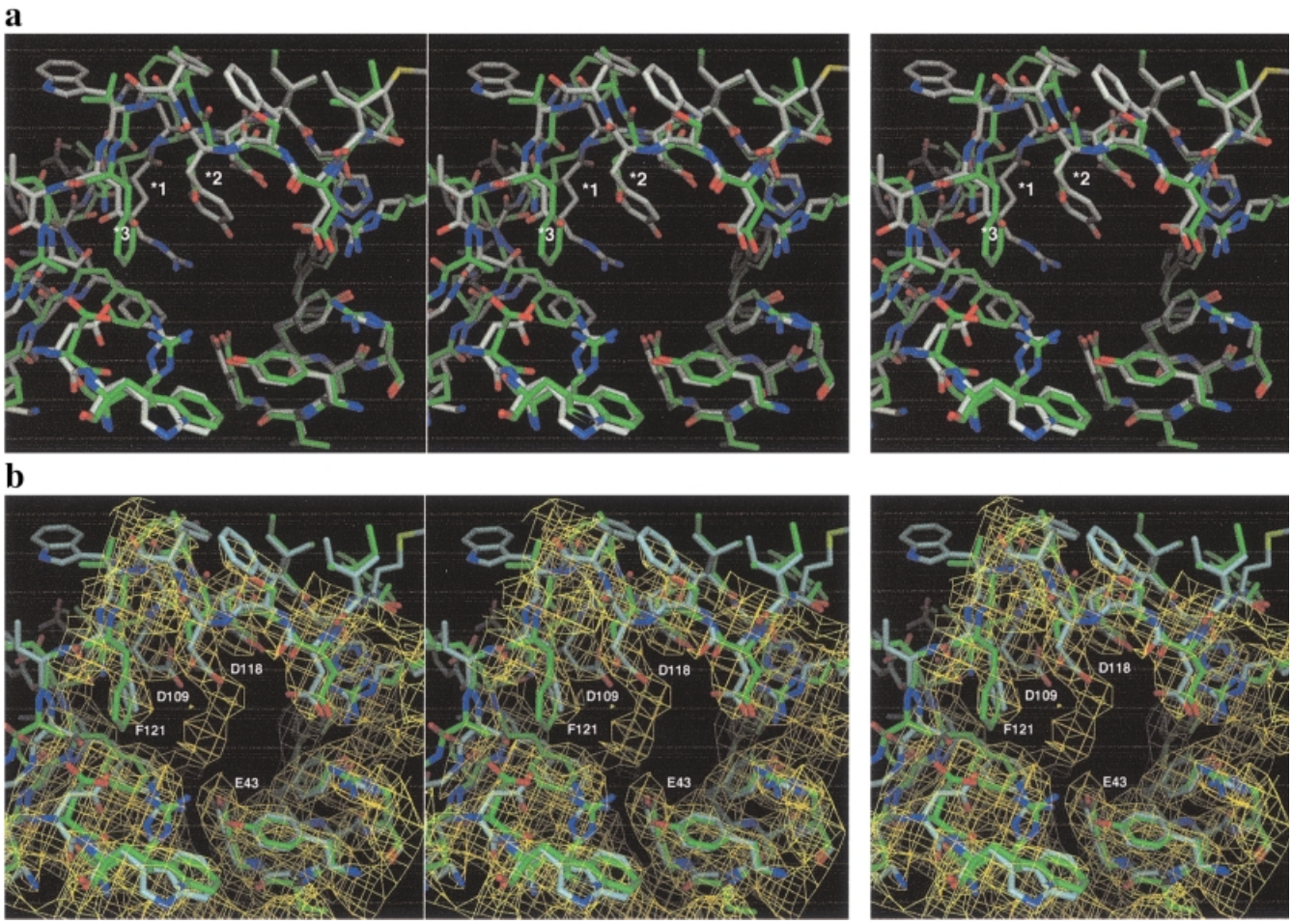

Fig. 1. (**a**) Stereo view of the superposition of the crystal structures of LamB (Schirmer *et al.*, 1995) and the ScrY–sucrose complex (carbon atoms shown in green) (Forst *et al.*, 1998). Shown is a cross-section of the channel at the height of the channel constriction. The view is from the extracellular side. Part of the greasy slide can be seen at the lower left. Loop L3 extends at the top of the figure. Most of the residues of the channel lining are identical except those at site *1, R109 (LamB), N192 (ScrY, partly buried within L3); site *2, F118 (LamB), D201(ScrY); and site *3, D121 (LamB), F204 (ScrY). (**b**) Superposition of the crystal structures of LamB mutant LamBY.1 and ScrY (carbon atoms in green). The cyclic averaged electron density of the mutant (contoured at 1.5σ) is shown superimposed on the structures. The density within the channel has not been modelled and may represent a cation and a water molecule.

interact with their respective substrates in LamB and ScrY (Dutzler *et al.*, 1996; Forst *et al.*; 1998).

Recently, the above-mentioned residues have been replaced by their LamB equivalents in ScrY (Ulmke *et al.*, 1999). The *in vivo* analysis showed that maltose transport was not significantly improved, while sucrose translocation was impaired.

This study aimed to render LamB permeable for sucrose. The initial mutant design was based on the knowledge of the LamB structure and a LamB–ScrY sequence alignment resulting in the triple mutant LamBY.1 (R109D, Y118D, D121F). Structural superposition of the two wild-type proteins (Figure 1a) performed later when the ScrY structure became available revealed that ScrY residue N192 instead of D191 is the structural homologue of R109. Therefore, a second triple mutant (LamBY.2; R109N, Y118D, D121F) was generated. Finally, in a third mutant (LamB.RY; R109A, Y118A), two bulky residues that contribute substantially to the LamB channel constriction were pruned to alanines.

Materials and methods

Strains and plasmids

All porins were expressed in *E.coli* strain BL21(DE3)omp5(Δ*lamB*, *ompR*) (Prilipov *et al.*, 1998). Construction of plasmid pGLamB and pGOmpF, containing the pMB1 ori of replication and ampicillin resistance gene, was described previously (Prilipov *et al.*, 1998). Site-directed mutagenesis of LamB was performed by the mutagenesis method as described (Prilipov *et al.*, 1998), resulting in plasmid pGLamBY.1 (changes R109D, Y118D, D121F), pGLamBY.2 (changes R109N, Y118D, D121F) and pGLamB.RY (changes R109A, Y118A). Mutations were confirmed by DNA sequence analysis (Perkin-Elmer ABI prism, 310 genetic analyser). Plasmid pGScrY was constructed by cloning a PCR fragment containing the *scrY* gene from pCH186 (Hardesty *et al.*, 1991) into *Sal*I/*Bam*HI-digested pGLamB. All DNA manipulations were performed according to Sambrook *et al.* (Sambrook *et al.*, 1989).

Protein purification, crystallization and crystallography

Expression and purification of the proteins were performed as described for LamB (Prilipov *et al.*, 1998). Crystallization of the LamBY.1 mutant was performed according to Keller *et al.* (Keller *et al.*, 1994) with the protein concentration for crystallization raised from 6 to 8 mg/ml. Crystallization of mutant LamBY.2 (based on structural alignment with ScrY, when the structure became available) was not attempted, since it is functionally very similar to LamBY.1.

Diffraction data were collected with a MARRESEARCH

Table I. Crystallographic data for the LamBY.1 mutant

Number of crystals	1
X-ray source	Rotating anode
Resolution range (Å)	20–3.2
Unique reflections	43576 (3454)
*R*merge	13.1 (35.3)
Completeness (%)	88.5 (71.3)
R (%)	19.3 (28.0)
*R*free (%)	21.8 (33.7)
R.m.s.d. bonds (Å)	0.016
R.m.s.d. angles (°)	2.2

The space group is $C222_1$, with cell constants a = 129.8 Å, b = 211.9 Å and c = 217.3 Å. Values in parentheses are for the highest resolution shell (3.31–3.20 Å).

image plate at a rotating anode X-ray generator (Table I). Data were processed and scaled using the programs DENZO and SCALEPACK (Otwinowski, 1993). The crystal structure was solved by difference Fourier methods using the phases of native LamB. After rigid body refinement, cyclic averaging over the three monomers of the asymmetric unit was performed using the program DM (Cowtan and Main, 1996). Subsequently, the model was rebuilt using program O (Jones and Kjeldgaard,1993) and refined by torsion angle simulated annealing including a bulk solvent contribution using program XPLOR (Brünger, 1992).

The pore cross-sections of the various channels were calculated using a 1×1×1 Å grid. The channel coordinate of LamB was approximated by the crystallographic *z*-axis (the molecular 3-fold axis forms an angle of 7° with the *z*-axis). For a given coordinate *z*, the number of grid points within the channel having a distance >1.4 Å from the protein were counted. The channel of the double alanine mutant LamB.RY was modelled by truncation of the respective side chains of wild-type model. For the calculation of the cross-sectional area of ScrY, the model was first superimposed onto the LamB model.

Current fluctuation analysis and liposome swelling assay

Lipid bilayers were formed as described previously (Van Gelder *et al.*, 2000). Current fluctuation measurements were performed to derive the kinetic parameters of sugar transport. In the absence of sugar the ion current through open channels fluctuates around an average value called the 1/*f* noise contribution. Upon addition of sugar, additional current fluctuations will be introduced which reflect the on and off rates of sugar binding. Assuming a two-state channel (sugar bound or unbound), the fluctuations around the average ionic current value yield the Lorentzian power spectrum (Nekolla *et al.*, 1994; Andersen *et al.*, 1995) which is given by $S_\omega = S_0/1+ (\omega/\omega_c)^2$, where S_0, the plateau value at zero frequency, is given by $S_0 = (4i^2/k_{off}^2)K[M]/(1 + K[M])^3$, with i = current through a single channel, [M] = sugar concentration, k_{off} = dissociation constant and K = equilibrium constant given by $K = k_{on}/k_{off}$. The corner frequency, ω_c, the second parameter determining the Lorentzian, is the frequency at which the amplitude decays to $\frac{1}{2}S_0$. Fluctuation theory shows that this frequency is related to the inverse of the decay time and to the on and off rates of sugar binding (Nekolla *et al.*, 1994; Andersen *et al.*, 1995). The filtered output voltage was recorded on paper and also on a storage oscilloscope (LeCroy) equipped with a fast Fourier transform (FFT) module. FFT was performed with a rectangular window on the oscilloscope. Power spectrum densities were recorded with a resolution of 1 Hz from 1 to 5000 Hz and averaged 50–100 times. Prior to sugar addition, we recorded the background contribution (1/*f*) which was subtracted from the Lorentzian-type power spectrum. One disadvantage of this method is that productive binding of the solute cannot be distinguished from non-productive binding. The latter situation would involve binding and release of the solute from/to the same side of the channel without translocation of the solute.

Liposome swelling assays with 2 µg of purified protein were performed as described (Luckey and Nikaido, 1980). Raffinose was used to determine the isotonic sugar concentration, which was typically between 60 and 100 mM. Liposome swelling monitors translocation directly. Since these experiments are performed at saturating sugar concentrations, the off rate towards the interior of the liposome is measured. When comparing translocation rates through different channels, it has to be considered that the individual proteoliposome preparations may differ in the size distribution of the vesicles and in the number of incorporated channels.

Sugar transport assays

LB medium supplemented with ampicillin (100 µg/ml) was inoculated with *E.coli* strain BL21(DE3)omp5 expressing the various maltoporin mutants. The bacteria were harvested at late log phase, collected by a quick spin, extensively washed in M9 medium and redissolved in M9 medium. For the transport assay, 10 µl of [^{14}C]sucrose (ARC Chemical, specific activity 600 mCi/mmol) was added to 1.5 ml of the cell suspension and the final sugar concentration was adjusted to 1 µM with cold sucrose. At different time points after the addition of the sugar, 150 µl of the suspension were filtered through a glass microfibre filter (Whatman GF/C) and washed with 5 ml of M9 medium. The filters were dried for 10 min at 60°C and counted in a scintillation counter. The *in vivo* sugar uptake assay measures translocation rates directly, is performed at low (physiological) sugar concentration and, therefore, is sensitive to the on rate of the process. It has the advantage that the channels are obviously oriented unidirectionally.

Results

Crystal structure of the triple mutant LamBY.1

The crystal structure of LamBY.1 has been determined to 3.2 Å resolution by X-ray crystallography (Table I). The structure is virtually identical with that of wild-type LamB. Despite the moderate resolution of the data, the electron density at the pore constriction clearly accounts for the three side chain replacements (Figure 1b). The side chains of D109 and D118 are within H-bonding distance, and consequently one of the two residues has to be protonated. There is residual density found in the lumen of the channel that extends into the space occupied by Y118 in wild-type LamB. This density may be attributed to a cation, which would be stabilized by the adjacent carboxylates and a water molecule.

Superposition of the wild-type structures of LamB and ScrY (overall root-mean-square deviation 1.3 Å) (Forst *et al.*, 1998) shows that the loop L3 segment Y_{107}QRH (LamB) corresponds to D_{189}RDNF (ScrY), with the first and the last residues being structurally equivalent (Figure 1a). Thus, ScrY carries a one-residue insertion which causes R109 to have no close equivalent [the C_α-position of R109 (LamB) has a distance of 5.0 and 1.4 Å to D191 and N192 of ScrY, respectively]. Accordingly,

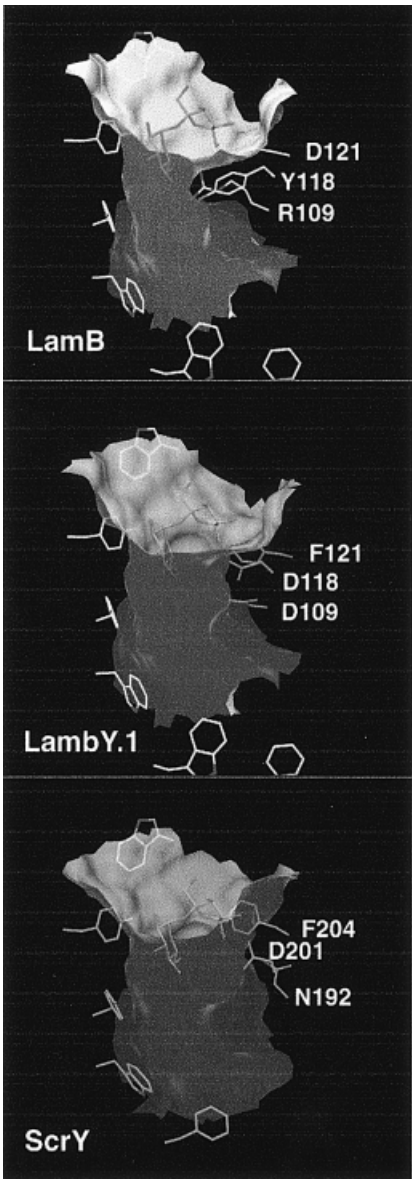

Fig. 2. Comparison of the channel shapes (visualized by the molecular surfaces) of LamB, LamBY.1 and ScrY. The outer surface of the molecules has been clipped off. The extracellular entrance to the channels is at the top of the figures. Residues of the 'greasy slide' and of the channel constriction are shown as stick models. The sucrose molecule is placed at the position as identified in the LamB-sucrose complex (Wang *et al.*, 1997). Figures 1 and 2 were generated with the program Dino (A.Philippsen, http://www.bioz.unibas.ch/~xray/dino).

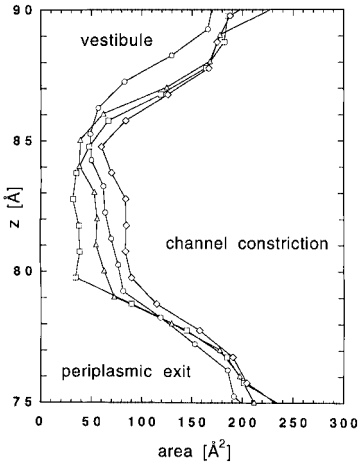

Fig. 3. Cross-sectional area of the central part of the porin channels measured as a function of the channel axis coordinate *z*. Squares, LamB; triangles, LamBY.1; circles, ScrY; diamonds, LamB.RY.

residue D109 of the mutant, which protrudes into the channel lumen, is at a different position compared with D191 or N192 of ScrY (Figure 1b). Side chains D118 and F121 of the mutant, however, show conformations similar to their counterparts in ScrY. The distances between the centres of the equivalent side chains are 1.8 and 1.0 Å, respectively.

In Figure 2, the channel shapes of the two wild-type proteins are compared with that of the mutant, and in Figure 3 the channel cross-sections are quantified. Compared with LamB, the pore cross-section of LamBY.1 is clearly increased. Replacement of D121 by the more bulky phenylalanine residue has no effect on the channel size, since the side chain is found remote from the constriction. At the constriction, the triple mutant pore is smaller than that of ScrY, mainly owing to the protruding residue D109 which is stabilized by an H-bond to D118 (Figure 1b). The structure of the double alanine mutant has been modelled by simply truncating the relevant side chains (R109A, Y118A). Based on this, the cross-section of the mutant channel even exceeds that of ScrY (Figure 3).

The reverse operation, replacement of ScrY porin residues by structurally equivalent LamB residues, has been performed recently (Ulmke *et al.*, 1999). As analyzed *in vivo*, the ScrY mutants did not exhibit an improved apparent transport K_m for maltose. Transport of sucrose, however, was considerably impeded, mainly owing to the D201Y mutation (which is the reverse of the Y118D mutation in LamB). The neutral effect of mutation N192R (which is the reverse of the R109D mutation in LamB) found by the authors may be due to a different side chain conformation which does not cause channel narrowing.

Transport characteristics of the various channels

Purified proteins were reconstituted into liposomes and the relative permeation rate of maltose and sucrose was determined by liposome swelling assay (Table II). Both wild-type channels, LamB and ScrY, show clear specificity for their respective substrates, with the permeation rates of sucrose through LamB and of maltose through ScrY at the detection limit as observed previously (Hardesty *et al.*, 1991). Both triple mutants, LamBY.1 and LamBY.2, showed a considerable increase in the relative sucrose permeation rate, approaching 20–25% of the maltose rate (Table II). Through the double mutant LamB-RY, sucrose permeation was even almost as efficient as maltose permeation. Also, the absolute swelling rates are drastically increased for sucrose, with the LamB.RY rate exceeding the ScrY rate (Table II). This demonstrates that the relative gain in sucrose permeation is not merely due to impaired maltose permeation, although translocation of maltose appears to be less efficient in the LamB mutants, probably owing to a slightly perturbed binding site at the channel constriction.

In vivo transport of sucrose

In vivo uptake of radiolabeled sucrose was measured to investigate the physiological relevance of the *in vitro* data. Since the ScrA and ScrB proteins that are required for sucrose transport across the cytoplasmic membrane and sucrose metabolism (Schmid *et al.*, 1988) were not provided, the assay reflects sugar permeation through the porins into the

Table II. Thermodynamic and kinetic data for maltose and sucrose transport through LamB, LamB mutants, ScrY and OmpF

Mutant	Sugar	k_{on} (10^3 M^{-1} s^{-1})	k_{off} (10^3 s^{-1})	K_d (mM)	$d(A/A_i)/dt$ (min^{-1})	ϕ_{rel} (%)
LamB	Maltose	270 ± 77	7.0 ± 1.5	25	0.234 ± 0.086	100
	Sucrose	1/*f*	1/*f*	15[a]	0.006 ± 0.008	2.7
LamBY.1	Maltose	40 ± 26	4.1 ± 0.4	105	0.124 ± 0.012	100
	Sucrose	1/*f*	1/*f*	–	0.031 ± 0.005	25
LamBY.2	Maltose	130 ± 25	7.9 ± 0.7	62	0.098 ± 0.015	100
	Sucrose	1/*f*	1/*f*	–	0.020 ± 0.007	21
LamB.RY	Maltose	110 ± 32	6.3 ± 1.6	57	0.171 ± 0.006	100
	Sucrose	120 ± 43	3.4 ± 0.6	28	0.133 ± 0.004	78
ScrY	Maltose	870 ± 148	6.9 ± 0.3	8	0.004 ± 0.008	4.5
	Sucrose	650 ± 135	9.0 ± 2.0	13	0.093 ± 0.025	100
OmpF	Maltose	1/*f*	1/*f*	–	nd[b]	75[c]
	Sucrose	1/*f*	1/*f*	–	nd[b]	100[c]

The rate constants k_{on} and k_{off} and the dissociation constant $K_d = k_{off}/k_{on}$ are the means of at least three measurements and $d(A/A_i)dt$ (with A_i = initial absorbance) and ϕ_{rel} values are the means of at least 10 measurements from at least three different proteoliposome preparations.
[a]Value derived from the stability constant $K = 67$ M^{-1} reported by Benz *et al.* (Benz *et al.*, 1987).
[b]Not determined.
[c]Values taken from Nikaido and Rosenberg (Nikaido and Rosenberg, 1981) with sucrose permeation set to 100%.

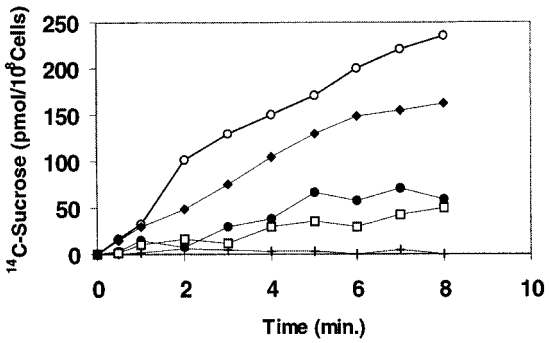

Fig. 4. Uptake of [^{14}C]sucrose into whole cells containing plasmids expressing the porins ScrY (open circles), LamB (crosses), LamBY.1 (closed circles), LamBY.2 (squares) and LamB.RY (diamonds). The concentration of sucrose in the medium was 1 μM.

periplasmic space. SDS–PAGE analysis showed that the various porins were equally well expressed (data not shown). As expected, the bacteria expressing wild-type LamB showed no sucrose uptake (Figure 4). In contrast, all three LamB mutants exhibited significant sucrose uptake, with the double mutant LamB.RY performing best and almost approaching the efficiency of the bacteria expressing wild-type ScrY.

Determination of kinetic parameters and binding affinities

Ion flow through LamB and ScrY is blocked upon sugar binding. Based on this, apparent on and off rates (k_{on}, k_{off}) of sugar binding can be derived by analysis of sugar-induced ion current noise (Nekolla *et al.*, 1994). The kinetic constants and the derived dissociation constants ($K_d = k_{off}/k_{on}$) of maltose and sucrose binding to the various porins are summarized in Table II. For wild-type LamB and the two triple mutants, the noise spectrum did not change upon addition of sucrose and no kinetic data could be derived (see Discussion). The same was observed in a control experiment with the non-specific OmpF porin.

Discussion

The outer membrane of Gram-negative bacteria contains several channel-forming proteins which allow the passage of solutes by passive diffusion. Most of them are non-specific and exclude solutes by size, whereas others contain a binding site for a particular compound. In this study, two such proteins were investigated, the maltooligosaccharide-specific LamB and the sucrose-specific ScrY porin. To confer sucrose specificity to LamB, two triple mutants were designed based on sequence and structural comparisons between LamB and ScrY, while the design of the double alanine mutant aimed for a channel with a large cross-section.

In agreement with earlier results (Luckey and Nikaido, 1980; Ulmke *et al.*, 1999), both translocation assays demonstrate that there is virtually no sucrose permeation through LamB. It has been demonstrated by X-ray structure analysis (Wang *et al.*, 1997) that the fructose moiety of sucrose is indeed too large to translocate through the LamB channel, whereas the glucose moiety inserts partly into the channel constriction and blocks the channel. The affinity constant of sucrose to LamB was measured to be 67 M^{-1} by sugar titration (Benz *et al.*, 1987). Sugar-induced noise analysis (Table II), however, did not reveal a change in the noise spectrum upon addition of the sugar. It appears likely that association/dissociation with and from the binding site, which is well accessible from the extracellular side, is too fast to be resolved by the instrumentation. Andersen *et al.* (1995, 1998) reported (very slow) rates for this process, which may reflect permeation events. It is not clear, however, how they were able to reveal sucrose-induced noise, while the sensitivity of their measurements was insufficient to measure maltose or even maltotriose rates.

The noise spectrum of the ion current through mutants LamBY.1 and LamBY.2 was not changed upon addition of sucrose. This may have the same reason as in the case above, i.e. that the kinetics are too fast to be resolved or may be due to absence of a binding site. The former possibility is contradicted by the significant permeation (Table II, Figure 4) measured in both translocation assays. The latter interpretation is supported by the fact that both R109 and D121, which form H-bonds with sucrose in the respective LamB complex (Wang *et al.*, 1997) and have been replaced in the mutants, are not available for sugar binding (Figure 2a). Also, the putative cation bound to D118 may hinder insertion of the glucose moiety into the constriction. Moreover, the newly introduced D109 may well interfere with binding, since it protrudes into the lumen, whereas the corresponding ScrY residue N192 is interacting with loop L3 and is not obstructing the channel.

Furthermore, D118 is extending more into the channel lumen than D201 of ScrY owing to a shift in the backbone. We propose that for steric reasons (obstruction by residues 109 and 118), the sugar has to tilt and its glucosyl moiety cannot stay in contact with the greasy slide, thus explaining the absence of defined kinetic constants in the current noise measurements. Hence the triple mutants behave more like general diffusion channels. Also in the case of the non-specific diffusion transport of maltose through OmpF no defined binding kinetics could be determined (Table II). These results nicely show the importance of the greasy slide as a key component of the binding site and are in line with recent results obtained by mutagenesis of greasy slide residues (unpublished data). It also demonstrates that the binding site for a non-permeable sugar such as sucrose is still present (see also crystal structure of the wild-type LamB-sucrose complex) (Wang *et al.*, 1997) and suggests that discrimination of solute transport is mainly based determined by the steric barrier at the constriction site.

If it were true that residues 109 and 118 of the triple mutants are interfering with sucrose binding, their truncation should result in free access to the greasy slide. Indeed, truncation of these residues to alanine in mutant LamB.RY appears to restore a binding site for sucrose with well-defined kinetics (Table II). The channel binds sucrose and maltose with comparable affinity, probably mainly via interactions between the glucose moiety and the channel lining. The dissociation constants are larger than the corresponding wild-type LamB values by only a factor of ~2 (Table II). Under liposome swelling conditions, the mutations render the channel about equally permeable to maltose and sucrose. The *in vivo* assay reveals an uptake rate as high as ~75% of the rate through ScrY.

In conclusion, the results show that wild-type LamB is impermeable to sucrose owing to steric hindrance at the channel constriction as directly revealed by the crystal structure of the complex (Wang *et al.*, 1997). In the triple mutants, this block is partly removed, but association of the sugar with the channel is still impeded, as evidenced by the absence of defined binding kinetics. However, in the truncation mutant, all obstacles are cleared and sucrose is transported almost as efficiently as maltose. Binding kinetics are now observed, most probably reflecting association with the greasy slide. For efficient transport of solutes comprised (partly) of glucosyl residues, unimpaired interaction with the greasy slide appears to be crucial, whereas the lack of ionizable residues may be tolerated in certain instances (the translocation efficiency of maltose through the truncation mutant is almost wild-type like). In most cases, however, mutagenesis of ionic track residues severely impedes the efficiency of the channel (Dumas *et al.*, 2000).

In this context, the poor efficiency of ScrY for maltose (Table II) is intriguing. Probably, owing to a non-optimal arrangement, the polar ScrY–maltose interactions are not strong enough to promote shedding of the sugar hydration shell. An analogous mechanism has been proposed for ion channels to explain ion selectivity (Doyle *et al.*, 1998).

Acknowledgements

We thank J.DiRienzo for providing plasmid pCH186, I.Bartoldus for the experiments with OmpF, A.Prilipov for construction of plasmid pGLamBY.1 and M.Winterhalter for technical support with the noise measurements. This work was sponsored by grant No. 31-53727.98 from the Swiss National Science Foundation to T.S. R.K was supported by grants Ko1686/3-1 and /3-2 from the Deutsche Forschungsgemeinschaft.

References

Andersen,C., Jordy,M. and Benz,R. (1995) *J. Gen. Physiol.*, **105**, 385–401.
Andersen,C., Cseh,R., Schülein,K. and Benz,R. (1998) *J. Membr. Biol.*, **164**, 263–274.
Benz,R., Schmid,A. and Vos-Scheperkeuter,G.H. (1987) *J. Membr. Biol.*, **100**, 21–29.
Brünger,A.T. (1992) *X-plor Version 3.1. A System for X-ray Crystallography and NMR*. Yale University Press, New Haven, CT.
Cowtan,K.D. and Main,P. (1996) *Acta Crystallogr.*, **D52**, 43–48.
Doyle,D.A., Cabral,J.M., Pfuetzner,R.A., Kuo,A., Gulbis,J.M., Cohen,S.L., Chait,B.T. and MacKinnon,R. (1998) *Science*, **280**, 69–77.
Dumas,F., Koebnik,R., Winterhalter,M. and Van Gelder,P. (2000). *J. Biol. Chem.*, **275**, 19747–19751.
Dutzler,R., Wang,Y.-F., Rizkallah,P.J., Rosenbusch,J.P. and Schirmer,T. (1996) *Structure*, **4**, 127–134.
Forst,D., Welte,W., Wacker,T. and Diederichs,D. (1998) *Nature Struct. Biol.*, **5**, 37–46.
Hardesty,C., Ferran,C. and DiRienzo,J.M. (1991) *J. Bacteriol.*, **173**, 449–456.
Jones,T.A. and Kjeldgaard,M. (1993) *O Version 5.9, The Manual.* Uppsala University, Uppsala.
Keller,T.A., Ferenci,T., Prilipov,A. and Rosenbusch,J.P. (1994) *Biochem. Biophys. Res. Commun.*, **199**, 767–771.
Koebnik,R., Locher,K.P. and Van Gelder,P. (2000) *Mol. Microbiol.*, **37**, 239–253.
Luckey,M. and Nikaido,H. (1980) *Proc. Natl Acad. Sci. USA*, **77**, 165–171.
Nekolla,S., Andersen,C. and Benz,R. (1994) *Biophys. J.*, **66**, 1388–1397.
Nikaido,H. and Rosenberg,E.Y. (1981) *J. Gen. Physiol.*, **77**, 121–135.
Nikaido,H. and Vaara,M. (1985) *Microbiol. Rev.*, **49**, 1–32.
Otwinowski,Z. (1993) In Sawyer,L. and Bailey,S. (eds), *Data Collection and Processing*. Science and Engineering Research Council Daresbury Laboratory, Daresbury, pp. 56–62.
Prilipov,A., Phale,P.S., Van Gelder,P., Rosenbusch,J.P. and Koebnik,R. (1998) *FEMS Microbiol. Lett.*, **163**, 65–72.
Randall-Hazelbauer,L. and Schwartz,M. (1973) *J. Bacteriol.*, **116**, 1436–1446.
Sambrook,J., Fritsch,E.F. and Maniatis,T. (1989) *Molecular Cloning. A Laboratory Manual.* 2nd edn. Cold Spring Harbor Laboratory Press, Cold Spring Harbor, NY.
Schirmer,T., Keller,T.A., Wang,Y.-F. and Rosenbusch,J.P. (1995) *Science*, **267**, 512–514.
Schmid, K, Ebner,R., Altenbuchner,J., Schmitt,R. and Lengeler,J.W. (1988) *Mol. Microbiol.*, **2**, 1–8.
Schmid,K., Ebner,R., Jahreis,K., Lengeler,J.W. and Titgemeyer,J. (1991) *Mol. Microbiol.*, **5**, 941–950.
Schülein,K., Schmid,K. and Benzl,R. (1991) *Mol. Microbiol.*, **5**, 2233–2241.
Schülein,K., Andersen,C. and Benz,R. (1995) *Mol. Microbiol.*, **17**, 757–767.
Szmelcman,S. and Hofnung,M. (1975) *J. Bacteriol.*, **124**, 112–118.
Szmelcman,S., Schwartz,M., Silhavy,T.J. and Boos,W. (1976) *Eur. J. Biochem.*, **65**, 13–19.
Ulmke,C., Kreth,J., Lengeler,J.W., Welte,W. and Schmid,T. (1999) *J. Bacteriol.*, **181**, 1920–1923.
Van Gelder,P., Dumas,F., Rosenbusch,J.P. and Winterhalter,M. (2000) *Eur. J. Biochem.*, **267**, 79–84.
Wang,Y.-F., Dutzler,R., Rizkallah,P.J., Rosenbusch,J.P. and Schirmer,T. (1997) *J. Mol. Biol.*, **272**, 56–63.

Received March 16, 2001; revised August 2, 2001; accepted August 9, 2001